

Sensitivity analysis of helical steam generator performance to primary side representative mass flux calculation methods

Jun Ha Hwang^a, Seung Hwan Oh, Doh Hyeon Kim, Semin Joo, Jeong Ik Lee^{a*}

^aDepartment of Nuclear and Quantum Engineering, Korea Advanced Institute of Science and Technology, 373-1 Guseong-dong Yuseong-gu, Daejeon 305-701, Republic of Korea

*Corresponding author: jeongiklee@kaist.ac.kr

***Keywords** : helical steam generator, heat transfer, sensitivity, modeling

1. Introduction

In the case of nuclear power plants, helical steam generators have emerged as the preferred option for fourth-generation reactors, including small modular reactors (SMRs), due to their capacity to minimize volume with high heat transfer density.

In recent studies on helical steam generators, the heat transfer performance has been evaluated by numerical methods [3, 8&13]. Among them, the heat transfer in the primary side (i.e. shell side) is one of the most important factors that determine the volume, thus it needs to be discussed from different perspectives of reflecting geometry. However, numerical modelling of helical steam generators for the primary side is currently using the Zukauskus straight horizontal tube heat transfer correlation.

This study presents an alternative approach to the calculation of the Reynolds number in the conventional Zukauskus heat transfer correlation by re-evaluating the maximum mass flux in the correlation. The modification is based on the discussion of helical steam generator geometry which is different from the straight horizontal tube geometry. Furthermore, by comparing the original Zukauskus correlation and modified version, further insight to the modelling of primary heat transfer in helical steam generators can be provided.

2. Methodology

In this section, the helical steam generator geometry design and operating conditions are discussed. The computation model used to design HSG and modified calculation methods are also illustrated.

2.1 Helical Steam Generator Design Approach

In the type of helical steam generator (HSG) considered in this study, the heated coolant flows from the center of the reactor module and heat transfer is achieved through eight steam generators contained in eight cassettes, as shown in Fig. 1. Therefore, the primary flow rate of each helical steam generator can be determined from the area of the cassette, and the total volume of the helical steam generator is approximately calculated from the product of the height along the

effective heat transfer length of the tube and the area of the cassette.

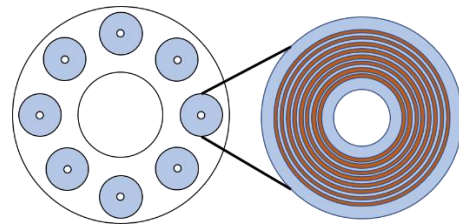


Fig. 1. A cross-sectional view of the integrated module reactor and the helical tube inside the cassette.

2.2 Thermal Design of HSG

In the helical steam generator (HSG), the heat transfer mechanisms within each cross-sectional plane are: convective heat transfer from hot side, conductive heat transfer through the tube wall, and convective heat transfer from cold side. The tube is discretized into meshes along its length. Shell and tube sides are interconnected for each mesh as shown in Fig. 2.

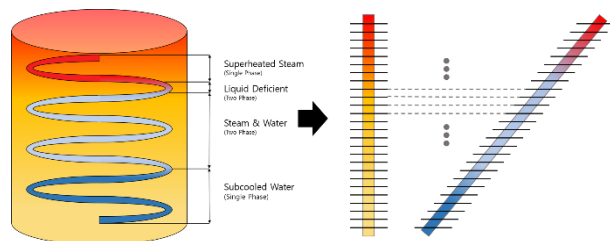


Fig. 2. Mesh discretization of helical steam generator

The computational model for heat transfer within the helical steam generator (HSG) employs a correlation that accounts for the pressure and temperature of each mesh. The iterative process begins by setting an initial estimate for the tube wall temperature derived from the adjacent coolant temperatures. Subsequently, this temperature estimate is refined by calculating the total thermal resistance. Upon convergence of the tube wall temperature, the resulting heat transfer is incorporated into the enthalpy of the fluid in subsequent mesh. This calculation continues iteratively and terminates upon reaching the final mesh, as depicted in Fig. 3.

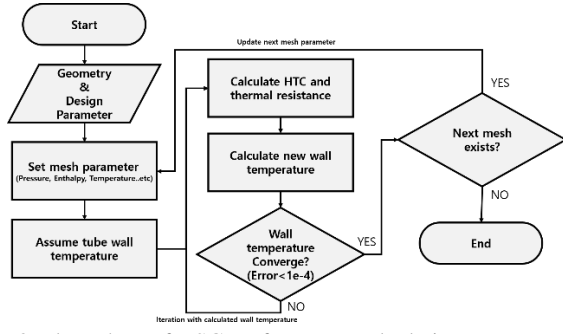


Fig. 3. Flow chart of HSG performance calculation

The primary side is regarded as a horizontal tube by using correlation of (Eq.1) Zukauskas [6] for crossflow heat transfer. On the secondary side, the model includes both single-phase and two-phase heat transfer, employing (Eq.2) Schmidt [5] for single-phase liquid heat transfer, (Eq.3) Chen [7] for two-phase flow, (Eq.5) Mori-Nakayama [2] for gas-phase heat transfer, and (Eq.4) Miropolskiy [11] for liquid-deficient areas after the dryout point, which is calculated by (Eq.6) Santini [4].

$$h_{Zukauskas} = CRe_i^m Pr_i^{0.36} \left(\frac{Pr_i}{Pr_w} \right)^{0.25} \frac{k_f}{d_o} \quad (1)$$

$$h_{Schmidt} = \left[0.023 \left\{ 1 + 3.6 \left(1 - \frac{d}{D} \right) \left(\frac{d}{D} \right)^{0.8} \right\} Re^{0.8} Pr^{\frac{1}{3}} \right] \frac{k}{d} \quad (2)$$

$$h_{chen} = h_{mac} F + h_{mic} S \quad (3)$$

$$h_{Miropolskiy} = 0.023 Y \frac{k_f}{d} \left(\frac{Gd}{\mu_g} \right)^{0.85} \left[x + \frac{\rho_g}{\rho_l} (1-x) \right]^{0.85} Pr_w^{0.8} \left(\frac{d}{D} \right)^{0.01} \quad (4)$$

$$Y = 1 - 0.1 \left(\frac{\rho_l}{\rho_g} - 1 \right)^{0.4} (1-x)^{0.4}$$

$$h_{Mori} = 0.03846 \frac{k_f}{d} Re^{0.8} \frac{Pr}{\left(Pr^{\frac{2}{3}} - 0.074 \right)} \left(\frac{d}{D} \right)^{\frac{1}{10}} \left[1 + \frac{0.098}{\left\{ Re \left(\frac{d}{D} \right)^2 \right\}^{\frac{1}{5}}} \right] \quad (5)$$

$$x_{dryout, santini} = (0.44 - 0.006P)G^{0.114} \quad (6)$$

* P unit is MPa

Pressure drop calculations on the primary side use the (Eq.7) Gilli [9] for single-phase. On the secondary side, (Eq.8) Ito [1] determines the friction coefficient for single-phase flow, while (Eq.9) Colombo [10] is used for two-phase flow multiplication factor.

$$\Delta P_{Gilli} = \frac{C_i C_n G^2}{\bar{f}_{eff} 2 \rho_{85}} \quad (7)$$

$$\bar{f}_{eff} = \frac{f'_{in-line} + 2f'_{staggered}}{2}, \quad f' = f \text{ from straight tube banks}$$

$$f_{Ito} = \left(\frac{d}{D} \right)^{0.5} \left[0.029 + 0.304 \left\{ Re \left(\frac{d}{D} \right)^2 \right\}^{-0.25} \right] \quad (8)$$

$$\Delta P = f_{Ito} \frac{L \rho v^2}{D} \frac{1}{2}$$

$$\Phi_{Colombo} = 0.0986 \left(1 + \frac{20}{X_{tt}} + \frac{1}{X_{tt}^2} \right) De^{0.19} \left(\frac{\rho_m}{\rho_l} \right)^{-0.4} \quad (9)$$

$$\Delta P = f_{Ito} \frac{L \rho v^2}{D} \frac{1}{2} \Phi_{Colombo}$$

2.3 HSG Model performance evaluation

The Schmidt heat transfer correlation for liquid single-phase section in the secondary side was evaluated through comparison with the experimental data obtained from Santini's 2015 studies. These experiments encompassed a range of conditions including variations in helical tube pressures, fluid mass fluxes, and heat fluxes under DC heating. The correlation's consistency with experimental data is particularly strong at higher heat fluxes and fluid mass fluxes, maintaining accuracy up to the threshold of dryout as depicted in Fig. 4.

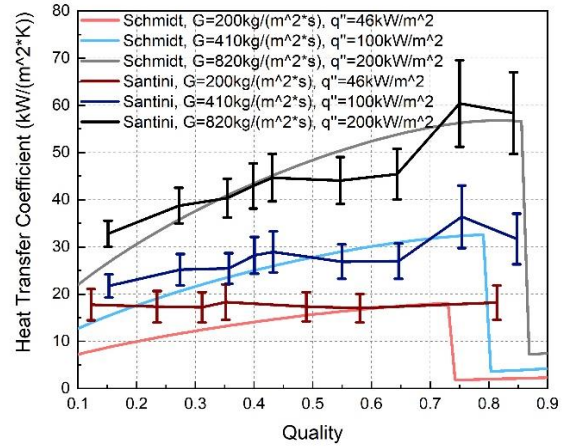


Fig. 4. Comparison at different mass flux and wall heat flux conditions at 6 MPa pressure

2.4 Modification of Zukaskus calculation

In the conventional method proposed by Zukaskus for evaluating heat transfer within horizontal tubes, the Reynolds number is determined using the flow velocity through the minimum cross-sectional area and the tube's external diameter as the characteristic length. This approach accounts for the dynamic changes in the area and velocity of the fluid flowing through the horizontal tube. This is due to the non-uniform configuration typically seen in horizontal tubes, as illustrated in Fig. 5. However, treating the helical coil as a horizontal circular tube necessitates a different methodology to calculate the maximum flow velocity. As depicted in Fig. 6, the inclination angle of the helical tube within a helical steam generator generates constant area and constant flow rate at each and every cross-section. The maintenance and rotation of the cross-sectional area as a function of height for single and multiple tubes, respectively, can be seen in the first and second rows.

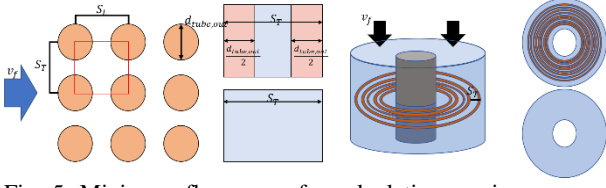


Fig. 5. Minimum flow areas for calculating maximum mass fluxes based on different type of tube array

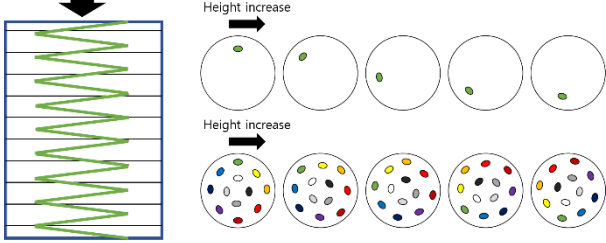


Fig. 6. Cross-sectional area of a helical tube based on height.

Thus, the Reynolds number calculations employing Zukaskus approaches can be tested with: the traditional Zukaskus method for computing the Reynolds number (Eq. 10), a method that calculates the Reynolds number based on the maximum mass flux while accounting for the geometry of the helical steam generator (Eq. 11), and a method that determines the Reynolds number using a constant mass flux (Eq. 12).

$$Re = \frac{G d_o}{\mu} \left(\frac{S_T}{S_T - d_o} \right) = \frac{G_{max} d_o}{\mu} \quad (10)$$

$$G = \frac{\dot{m}}{A_{cassete}}, \quad A_{cassete} = \frac{\pi}{4} (D_{Cassete,o}^2 - D_{Cassete,i}^2)$$

$$Re = \frac{G d_o}{\mu} \left(\frac{A_{cassete}}{A_{cassete} - A_{max,coil}} \right) = \frac{G_{max} d_o}{\mu} \quad (11)$$

$$A_{max,coil} = \frac{\pi}{4} \sum_{j=1}^n \{ (D_{coil,j} + d_o)^2 - (D_{coil,j} - d_o)^2 \}$$

$$Re = \frac{G_{const} d_o}{\mu} \quad (12)$$

$$G_{const} = \frac{\dot{m}}{A_{const}}$$

$$A_{const} = \frac{\left\{ \frac{\pi}{4} (D_{Cassete,o}^2 - D_{Cassete,i}^2) H_{coil} - N_{tube} \frac{\pi}{4} d_{tube,o}^2 L_{coil} \right\}}{H_{coil}}$$

3. Result and Discussions

The assumed design conditions for the helical steam generator are summarized in Table 1. The hypothetical conditions were determined by referencing to available information of MRX, IRIS, and SMART [3]. The geometry is designed with the model to achieve design conditions and it is presented in Table 2. It is noted that these conditions are held the same when evaluating the effect of changing the mass flux evaluation methods.

Table I: Operation Condition of HSG

Primary inlet flow rate [kg/s]	500
Secondary inlet flow rate [kg/s]	60
Primary inlet temperature [K]	600.4
Primary inlet pressure [MPa]	15

Secondary inlet temperature [K]	500
Secondary outlet pressure [MPa]	5
Primary outlet temperature [K]	560.0
Secondary outlet temperature [K]	573.15

Table II: Geometry Design of HSG

Number of tubes [m]	600
Tube thermal conductivity [W/m·K]	16
Inner diameter of tubes [m]	0.012
Outer diameter of tubes [m]	0.016
Tube length [m]	32.0
Coil number of tubes	19
Average helix angle [°]	10
Radial pitch [m]	0.025
Axial pitch [m]	0.025
Innermost helical diameter [m]	0.65
Outermost helical diameter [m]	1.55
Inner diameter of cassette [m]	1.6
Outer diameter of cassette [m]	0.6

Within the framework of Zukaskus correlation, the outcomes derived from the specific geometry and operating conditions using conventional maximum mass flux (Eq. (10)), modified maximum mass flux (Eq. (11)), and constant mass flux method (Eq. (12)) are summarized in Table 3.

Table III: Calculation result of each mass flux method

Case	Eq. 10	Eq. 11	Eq. 12
Tube length [m]	33.06	33.49	35.72
Two-phase region [m]	23.25	23.63	25.2
Dryout point [m]	28.18	28.26	30.37

The findings indicate that variations in the Reynolds number due to different mass fluxes require different tube lengths to achieve design conditions. The highest heat transfer was predicted when considering the maximum flow rate for straight horizontal tubes as originally suggested in Zukaskus correlation.

Fig. 7 illustrates the sensitivity of the secondary helical tube length to the chosen mass flux calculation method. Only the outer diameter of the helical steam generator is increased. As the shell outer diameter increases, the primary flow area increases, resulting in a decrease in mass flux under conditions of constant mass flow. The lower mass flux on the primary side leads to a decrease in the Reynolds number, which results in a lower primary side heat transfer coefficient, i.e. decreased heat transfer and increased tube length. Notably, the sensitivity to changes in the shell outer diameter is most pronounced when employing the modified maximum mass flux method and least significant when utilizing the original Zukaskus maximum mass flux calculation method.

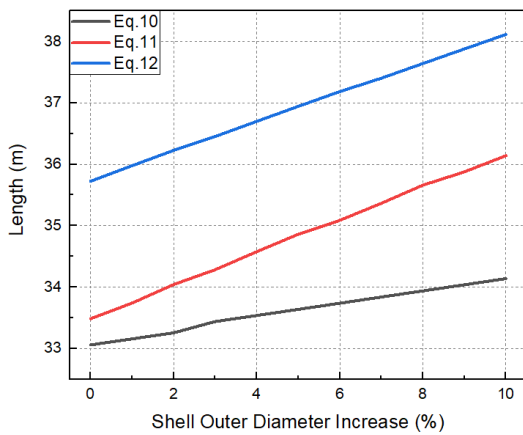


Fig. 7. Secondary tube length when shell diameter increase

4. Summary and Further Works

This study assessed how different way of calculating the mass flux for shell side (i.e. primary side in nuclear system) heat transfer in a helical steam generator affect the heat exchanger design and analysis. It is shown that the shell side mass flux calculation affects not only the shell geometry but also the helical tube (i.e. secondary side in nuclear system) length to the heat transfer capacity.

The results shows that assuming the constant mass flux on the primary side, which considers the inclination angle, provides the most conservative approach for evaluating the heat transfer performance of the helical steam generator model. Furthermore, the conventional Zukaskus heat transfer for horizontal tube shows less sensitivity of the changes in the helical tube length to the shell side diameter for meeting the design conditions.

Experimental data will be needed to determine which method is the most appropriate and further modification of heat transfer correlation, including exponents of the Reynolds number, for representing the helical steam generator heat transfer. However, since the shell side of helical steam generator includes complicated structure to support multiple tubes, and this will inevitably make the flow and heat transfer phenomenon more complex. Therefore, a generalized heat transfer or a friction factor correlation for a helical steam generator will probably have a limitation when it is applied to a practical problem. These factors have to be investigated in the future by collecting more experimental data in this area.

ACKNOWLEDGEMENT

This work was supported by the Innovative Small Modular Reactor Development Agency grant funded by the Korea Government (MOTIE) (No. RS-2024-00404240).

REFERENCES

[1] El-Genk, M. S., & Schriener, T. M. (2017). A review and correlations for convection heat transfer and pressure losses in

toroidal and helically coiled tubes. *Heat Transfer Engineering*, 38(5), 447-474.

[2] Mori, Y., & Nakayama, W. (1967). Study on forced convective heat transfer in curved pipes:(3rd report, theoretical analysis under the condition of uniform wall temperature and practical formulae). *International journal of heat and mass transfer*, 10(5), 681-695.

[3] Liu, K., Wang, M., Zhang, J., Guo, K., Tian, W., Qiu, S., & Su, G. H. (2023). Numerical investigation on the thermal load heterogeneity of multi-assembly helical coil steam generator in high temperature gas-cooled reactor. *Energy*, 281, 128355.

[4] Santini, L., Cioncolini, A., Lombardi, C., & Ricotti, M. (2014). Dryout occurrence in a helically coiled steam generator for nuclear power application. In *EPJ Web of Conferences* (Vol. 67, p. 02102). EDP Sciences.

[5] Schmidt, E. F. (1967). Wärmeübergang und druckverlust in rohrschlangen. *Chemie Ingenieur Technik*, 39(13), 781-789.

[6] Žkauskas, A. (1987). Heat transfer from tubes in crossflow. In *Advances in heat transfer* (Vol. 18, pp. 87-159). Elsevier.

[7] Chen, J. C. (1966). Correlation for boiling heat transfer to saturated fluids in convective flow. *Industrial & engineering chemistry process design and development*, 5(3), 322-329.

[8] Yao, H., Chen, G., Lu, K., Wu, Y., Tian, W., Su, G., & Qiu, S. (2021). Study on the systematic thermal-hydraulic characteristics of helical coil once-through steam generator. *Annals of Nuclear Energy*, 154, 108096.

[9] Gilli, P. V. (1965). Heat transfer and pressure drop for cross flow through banks of multistart helical tubes with uniform inclinations and uniform longitudinal pitches. *Nuclear Science and Engineering*, 22(3), 298-314.

[10] Colombo, M., Colombo, L. P., Cammi, A., & Ricotti, M. E. (2015). A scheme of correlation for frictional pressure drop in steam-water two-phase flow in helicoidal tubes. *Chemical Engineering Science*, 123, 460-473.

[11] Miropolskiy, Z. L. (1963). Heat transfer in film boiling of a steam-water mixture in steam-generator tubes. *Teplonergetika*, 10, 49-52.

[12] U.S. Department of Energy. IRIS International Reactor Innovative and Secure Final technical progress report.2023.

[13] Lian, Q., Tian, W., Gao, X., Chen, R., Qiu, S., & Su, G. H. (2020). Code improvement, separate-effect validation, and benchmark calculation for thermal-hydraulic analysis of helical coil once-through steam generator. *Annals of Nuclear Energy*, 141, 107333.